Chiral switching by spontaneous conformational change in adsorbed organic molecules

SIGRID WEIGELT[1], CARSTEN BUSSE[1]*, LARS PETERSEN[1], EVA RAULS[1], BJØRK HAMMER[1], KURT V. GOTHELF[2], FLEMMING BESENBACHER[1] AND TROLLE R. LINDEROTH[1]†

[1]Interdisciplinary Nanoscience Center at the University of Aarhus (iNANO), Department of Physics and Astronomy, University of Aarhus, DK-8000 Aarhus C, Denmark
[2]Interdisciplinary Nanoscience Center at the University of Aarhus (iNANO), Department of Chemistry, University of Aarhus, DK-8000 Aarhus C, Denmark
*Present address: Lehrstuhl für Physikalische Chemie I, Ruhr-Universität Bochum, D-44780 Bochum, Germany
†e-mail: trolle@inano.dk

Published online: 15 January 2006; doi:10.1038/nmat1558

Self-assembly[1,2] of adsorbed organic molecules is a promising route towards functional surface nano-architectures, and our understanding of associated dynamic processes has been significantly advanced by several scanning tunnelling microscopy (STM) investigations[3–7]. Intramolecular degrees of freedom are widely accepted to influence ordering of complex adsorbates, but although molecular conformation has been identified[8] and even manipulated[9–11] by STM, the detailed dynamics of spontaneous conformational change in adsorbed molecules has hitherto not been addressed. Molecular surface structures often show important stereochemical effects as, aside from truly chiral molecules[12–15], a large class of so-called prochiral molecules[16–19] become chiral once confined on a surface with an associated loss of symmetry. Here, we investigate a model system in which adsorbed molecules surprisingly[16] switch between enantiomeric forms as they undergo thermally induced conformational changes. The associated kinetic parameters are quantified from time-resolved STM data whereas mechanistic insight is obtained from theoretical modelling. The chiral switching is demonstrated to enable an efficient channel towards formation of extended homochiral surface domains. Our results imply that appropriate prochiral molecules may be induced (for example, by seeding) to assume only one enantiomeric form in surface assemblies, which is of relevance for chiral amplification and asymmetric heterogenous catalysis.

The molecule[20] investigated in this article is shown in Fig. 1a. It consists of a linear backbone formed from three benzene rings connected by ethynylene spokes, and is functionalized at both ends with an aldehyde, a hydroxyl and a bulky *t*-butyl group. Vapour deposition of this compound onto the inert herringbone reconstructed Au(111)-$(22 \times \sqrt{3})$ surface under ultrahigh-vacuum conditions results in two coexisting adsorption phases, as revealed by STM. In the phase shown in Fig. 1c–e, the molecules adsorb with their backbone parallel to the substrate and align into rows that are shifted relative to each other by half the repeat distance along the rows, analogous to the stacking in a brick wall. The contrast in the STM image of Fig. 1d is ascribed primarily to the conjugated π-system of the molecule. A spontaneous change of tip conditions can result in another imaging mode where the contrast is dominated by bright protrusions at the ends of the molecules, positioned off-axis with respect to the molecular backbone (Fig. 1c) and attributed to the *t*-butyl groups[5,7]. In contrast to the gas phase, where the molecule has freedom of rotation around the ethynylene spokes, the adsorbed molecule is confined by the substrate to assume distinct surface conformers, distinguishable[8,14,15] in the STM images by the position (right or left) of the bright *t*-butyl group with respect to the molecular backbone. As illustrated in Fig. 1b, three surface conformers result: one meso-form (LR/RL), which is achiral owing to a mirror plane perpendicular to its axis, and two chiral enantiomers (LL and RR), which cannot be brought to overlap by rotation and translation in the plane of the surface. All three types of conformer can be found in the brick-wall phase, as indicated in Fig. 1c.

From time-lapse sequences of STM images we find that the bright protrusions ascribed to *t*-butyl groups occasionally change position from one side of the molecular backbone to the other (see Supplementary Information for an example of an STM video). Such shifts are illustrated in Fig. 2a by superimposing two time-separated STM images of the same portion of the surface. The images have been coloured blue and orange, respectively, such that stationary protrusions appear grey, and blue (orange) indicates initial (final) positions of protrusions that have moved. On a given molecule, only one *t*-butyl group changes position at a time. We therefore interpret the observed shifts as resulting from an intramolecular conformational change in which one of the phenyl endgroups rotates around the axis of the ethynylene spoke, transferring the *t*-butyl group from one side of the molecular axis to the other (see Fig. 1a). (A small number of events in which the *t*-butyl groups at both ends of a molecule change position between consecutive images can be explained as uncorrelated, successive flips of the two

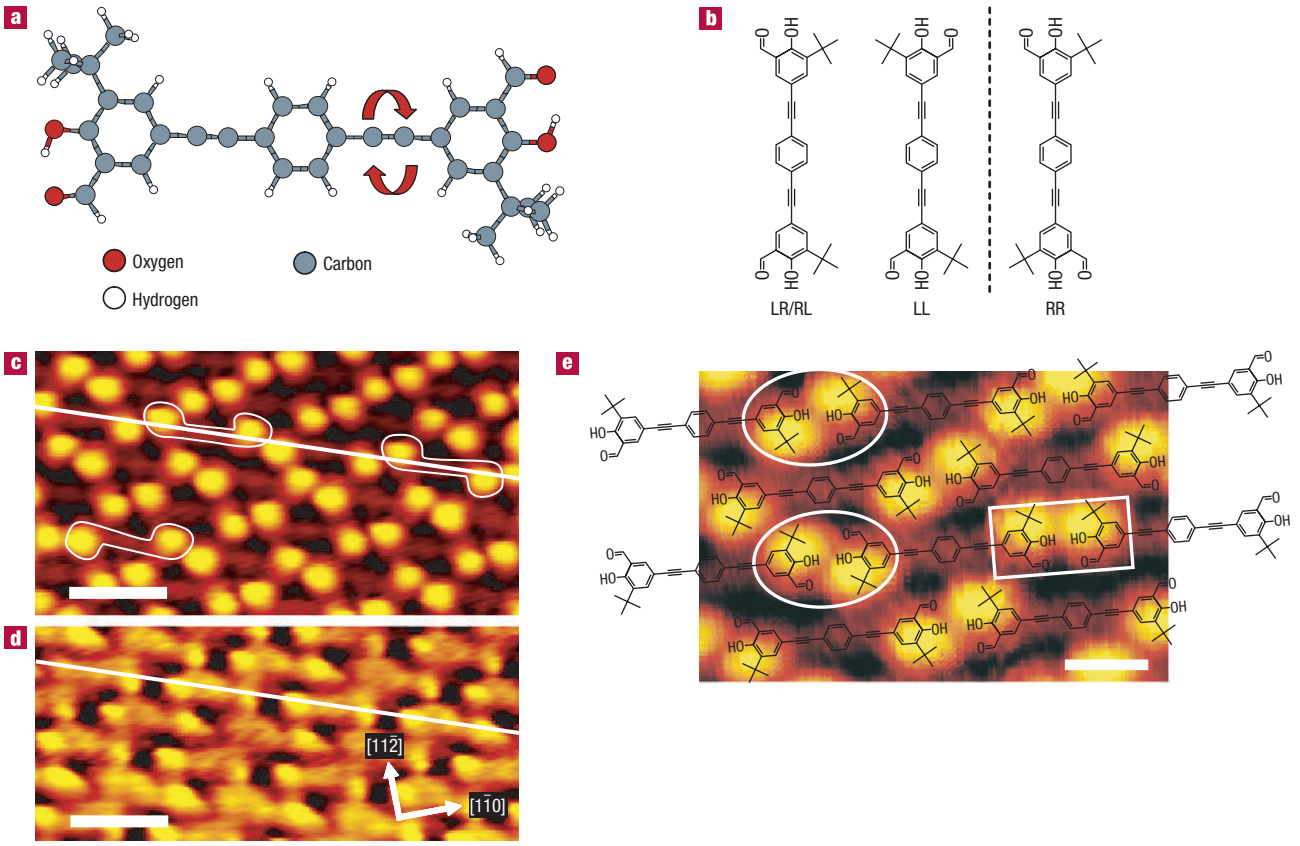

Figure 1 Brick-wall adsorption structure. a, Chemical structure of the investigated molecule. **b**, Three distinct surface conformers, two of which are enantiomers. R and L indicate the position (right and left) of the *t*-butyl group with respect to the molecular backbone as seen from the centremost benzene ring. **c**,**d**, Constant-current STM images of the brick-wall adsorption structure attained under tip conditions primarily revealing the *t*-butyl groups (**c**) and molecular π-system (**d**). Sample voltage -1 V, tunnel current 0.8 nA, scale bar 2 nm in both images. Molecular conformation is assigned based on the position of the bright protrusions in **c** with respect to the indicated line following the direction of the molecular backbones. Outlines of three surface conformers are shown in **c**. **e**, Schematic model of the brick-wall adsorption structure superimposed on an STM image. The *cis* and *trans* arrangements for endgroups on molecules meeting head-to-head are indicated by a rectangle and ellipses, respectively. Scale bar 1 nm.

molecular endgroups.) This spontaneous flipping process implies that the molecules are not completely stereochemically fixed by the substrate, but can change between the different surface conformers, specifically from chiral (RR/LL) to achiral (RL/LR) or *vice versa* by a rotation of one endgroup or between the two chiral enantiomers by a consecutive rotation of both endgroups.

The potential-energy landscape felt by a molecule during flipping is influenced by interactions with adjacent molecules. In particular, neighbouring endgroups on molecules that meet head-to-head along the rows of the brick-wall phase may assume either a *cis* arrangement, that is with their *t*-butyl groups at the same side of the molecular rows, or a *trans* arrangement, where the *t*-butyl groups are at opposite sides (see Figs 1e and 2b; note that in the present context, the terms *cis* and *trans* refer to an intermolecular rather than intramolecular arrangement). The *trans* arrangements dominate: only 7% *cis* arrangements are observed under equilibrium conditions at 197 K, corresponding to an energy difference between the two arrangements of 0.04 eV. This asymmetry is expected to yield a higher rate for molecular flips changing a *cis* arrangement to *trans* as compared with flips that change *trans* to *cis*, as illustrated in the schematic potential-energy contour of Fig. 2b. The potential-energy surface is also influenced by interactions between molecules in adjacent rows and intramolecular interactions between the two ends of a molecule, but these are weaker than the head-to-head interactions (as they are observed to lead to less ordering) and were not taken into account in our analysis.

The rates $\Gamma_{trans\text{–}cis}$ and $\Gamma_{cis\text{–}trans}$ have been determined from the analysis of STM videos acquired at a range of sample temperatures between 140 and 230 K, and are plotted in Fig. 2c. The *cis–trans* flips indeed occur with a higher rate than *trans–cis*. By fitting the two datasets to the Arrhenius expression, $\Gamma = \nu \exp(-E/k_B T)$, where ν is the pre-factor, E the activation energy, k_B is the Boltzmann constant and T the temperature, we obtain $E_{trans\text{–}cis} = (0.32 \pm 0.03)$ eV and $E_{cis\text{–}trans} = (0.28 \pm 0.03)$ eV, consistent with Fig. 2b and the determined energy difference between *cis* and *trans* pairs. The resulting pre-factors $\nu_{trans\text{–}cis} = 10^{5.8\pm0.8}$ s^{-1} and $\nu_{cis\text{–}trans} = 10^{6.1\pm0.8}$ s^{-1} are considerably smaller than the 'standard' $k_B T/h \sim 10^{12}$ s^{-1} (where h is Planck's constant) expected from transition-state theory and observed, for example, for molecular diffusion on surfaces[5,6]. This might be related to a lowering of the entropy in the transition state caused by a confinement of molecular degrees of freedom.

To illuminate the dynamics of the conformational change, we have performed modelling based on density functional theory. Calculations for the entire molecule on the Au surface are computationally unfeasible and hence we have only modelled the end portion of the molecule (Fig. 3a). As the two endgroups of a given molecule are observed to flip independently of each other, we assume that the remaining part of the molecule stays

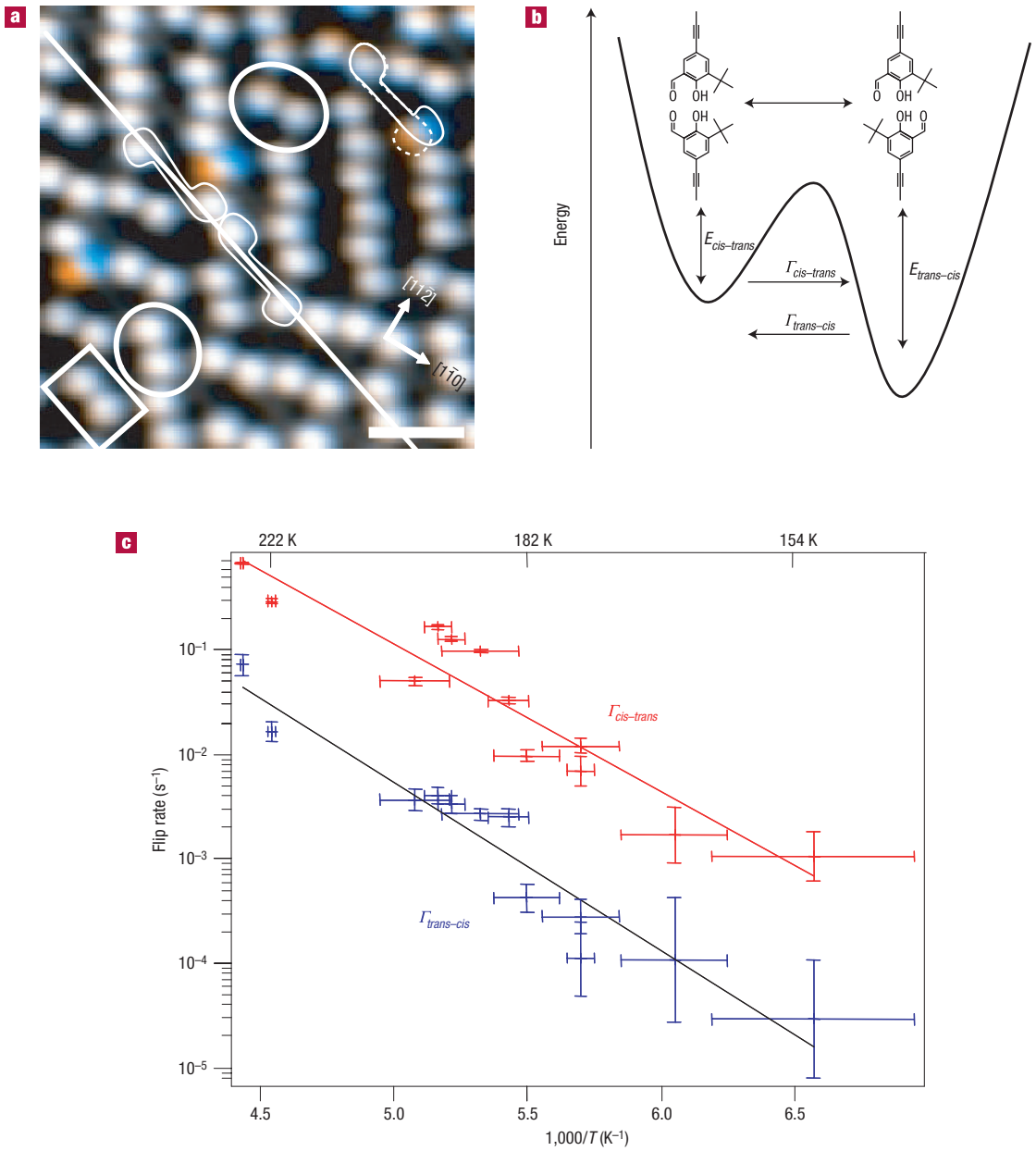

Figure 2 Conformational changes for molecules in the brick-wall structure. a, Overlay of two STM images taken with a time separation of 168 s (tunnel current 0.4 nA, sample voltage 1.96 V, sample temperature 180 K, scale bar 2 nm). Blue (orange) indicates the initial (final) positions of *t*-butyl groups that change position, whereas stationary groups appear grey. Two *cis–trans* and one *trans–cis* (rightmost in image) flips are shown. Outlines of three molecules are indicated as well as stationary *cis* (rectangle) and *trans* (circles) arrangements of endgroups. (The orientation of the image differs from Fig. 1, the indicated line follows the direction of the molecular backbones.) **b**, Schematic energy diagram of the *cis* and *trans* arrangements. **c**, Arrhenius plot of the rate for *cis–trans* and *trans–cis* flips. Horizontal error bars indicate the temperature interval over which the STM data used to evaluate the respective datapoints were acquired. Vertical error bars represent one standard deviation.

bound to the substrate during the conformational change. In the calculations, the influence from this part of the molecule on the modelled end portion is taken into account by constraining the carbon atom marked by an asterisk to be at the distance from the surface found to be optimum for a benzene molecule (3.48 Å). In the optimum adsorption configuration (Fig. 3a), the presence of the bulky *t*-butyl group leads to an 18° tilting of the benzene ring in the end portion, whereas in the transition state (Fig. 3b) the benzene ring is rotated to bring the *t*-butyl group away from the surface. The energy difference between the two configurations is 0.20 eV. In the transition state, the molecular axis is tilted by 25° away from the surface (see the inset in Fig. 3b) corresponding to a pronounced bending of the molecular backbone. To estimate the associated energy cost, we modelled the entire free molecule in similarly bent (Fig. 3c) and non-bent (not shown) transition-state configurations and found an energy difference between the two of 0.17 eV. In conclusion, the net energy barrier for the conformational change is therefore estimated from the calculations to be 0.37 eV, comparable to the experimental value, and is composed of two approximately equal contributions arising from a reduced molecule–surface interaction and bending strain in the molecule. For the free molecule, in comparison, we

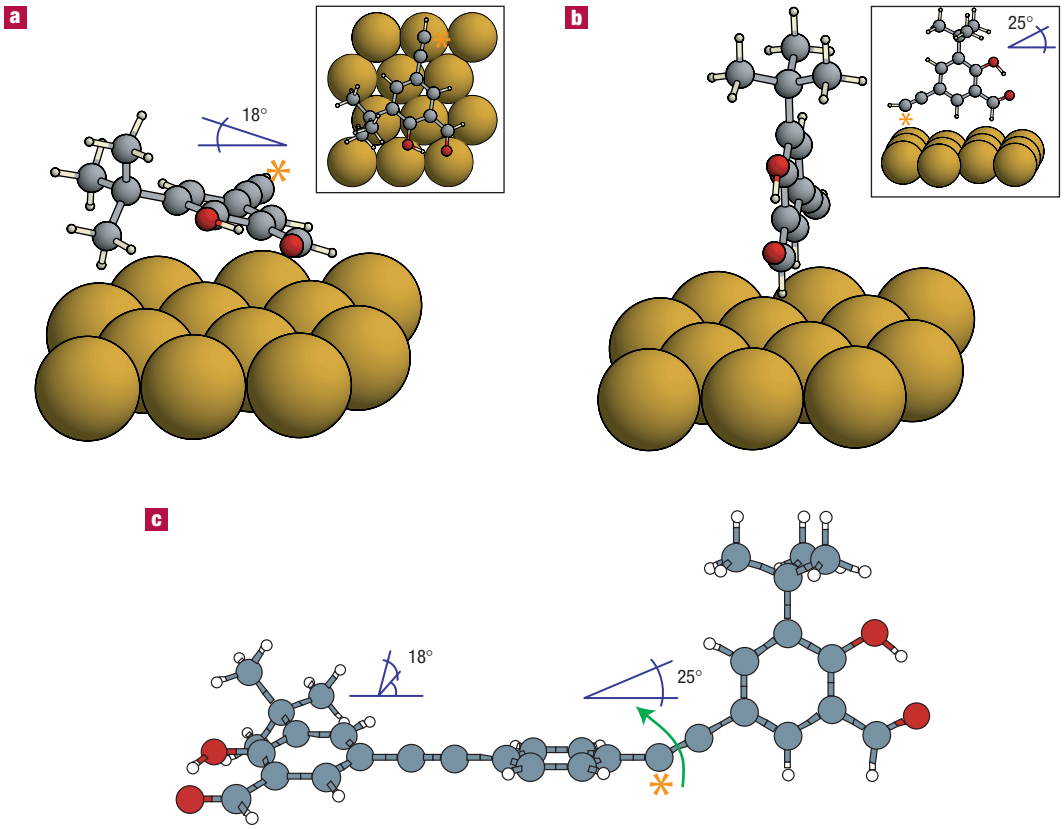

Figure 3 Structures from theoretical modelling. a, Optimum adsorption geometry for the molecular fragment. The carbon atom marked by an asterisk has been saturated by a hydrogen atom. Inset: top view. **b**, Optimum transition-state geometry. Inset: side view. **c**, Free molecule in a strained geometry with the backbone bent by 25° as suggested from **b**. (Note that not all gold atoms in the supercell used are shown in **a** and **b**.)

find that the barrier towards rotation around the ethynylene spoke is only 0.037 eV.

The observed conformational changes have implications for the chiral ordering on surfaces. This is appreciated by considering the second coexisting phase formed from the molecules, shown in Fig. 4a. The dominating motif is a windmill-like arrangement of four molecules adsorbed with their backbone parallel to the substrate and joined in a common node. Each molecule connects two adjacent nodes, producing an extended, ordered network with openings bound by four molecules. This tiling pattern is chiral as the windmill motif can be constructed in two mirror-image forms with an opposite sense of rotation (see Fig. 4a). The *t*-butyl groups are completely ordered in this network phase, as they are always positioned at the side of the molecular backbone pointing away from the central node. This introduces a correlation between the chirality of the tiling pattern and the chirality of the participating surface conformers: Each chiral form of the tiling pattern consists entirely of one of the two chiral surface conformers (LL/RR), as shown schematically in Fig. 4a. Large enantiopure domains are thus observed to form, as seen in the STM image of Fig. 4b showing two domains of opposite chirality. Figure 4c shows an overlay (see Fig. 2a) of two time-separated STM images acquired at the edge of a homochiral domain consisting of RR conformers. In the first image (blue) an achiral RL conformer, coming from the lattice gas at the left side of the image, has attached itself to the edge, and in the second image (orange) a conformational change has occurred, switching this molecule to the chiral RR conformer, enabling it to fit into the structure. This flip is estimated to occur with a rate comparable to that observed for molecules in the brick-wall phase, although the molecule is situated in a different environment. The molecules embedded in the chiral structure are not observed to undergo conformational changes, which we attribute to stronger intermolecular interactions in this structure compared with the brick-wall phase (possibly mediated by hydrogen bonding).

The ability to switch chirality by performing one or more conformational changes enables the molecules to accommodate to the chiral template found at the edge of the island and to incorporate themselves into homochiral domains. The chiral segregation[16–19] on surfaces of racemic mixtures formed from adsorbed prochiral compounds has been ascribed to lateral mass transport, sometimes over mesoscopic distances, in combination with chiral recognition/selection at the perimeters of enantiopure domains. The accommodation mechanism described here is a more effective channel towards chiral segregation on surfaces. The formation of homochiral adsorbate layers may be accomplished by seeding[21] the surface with an appropriate chiral template compound or by adsorbing the molecules on a chiral metal surface[22]. The potential ability of achiral molecules to form homochiral assemblies on surfaces is of interest for heterogeneous asymmetric catalysis and with respect to understanding the origin of the homochirality observed in nature.

METHODS

The experiments were performed in an ultrahigh-vacuum system equipped with the home-built variable-temperature Aarhus STM[23] (see also http://www.specs.de). The Au(111) surface was prepared by repeated cycles of

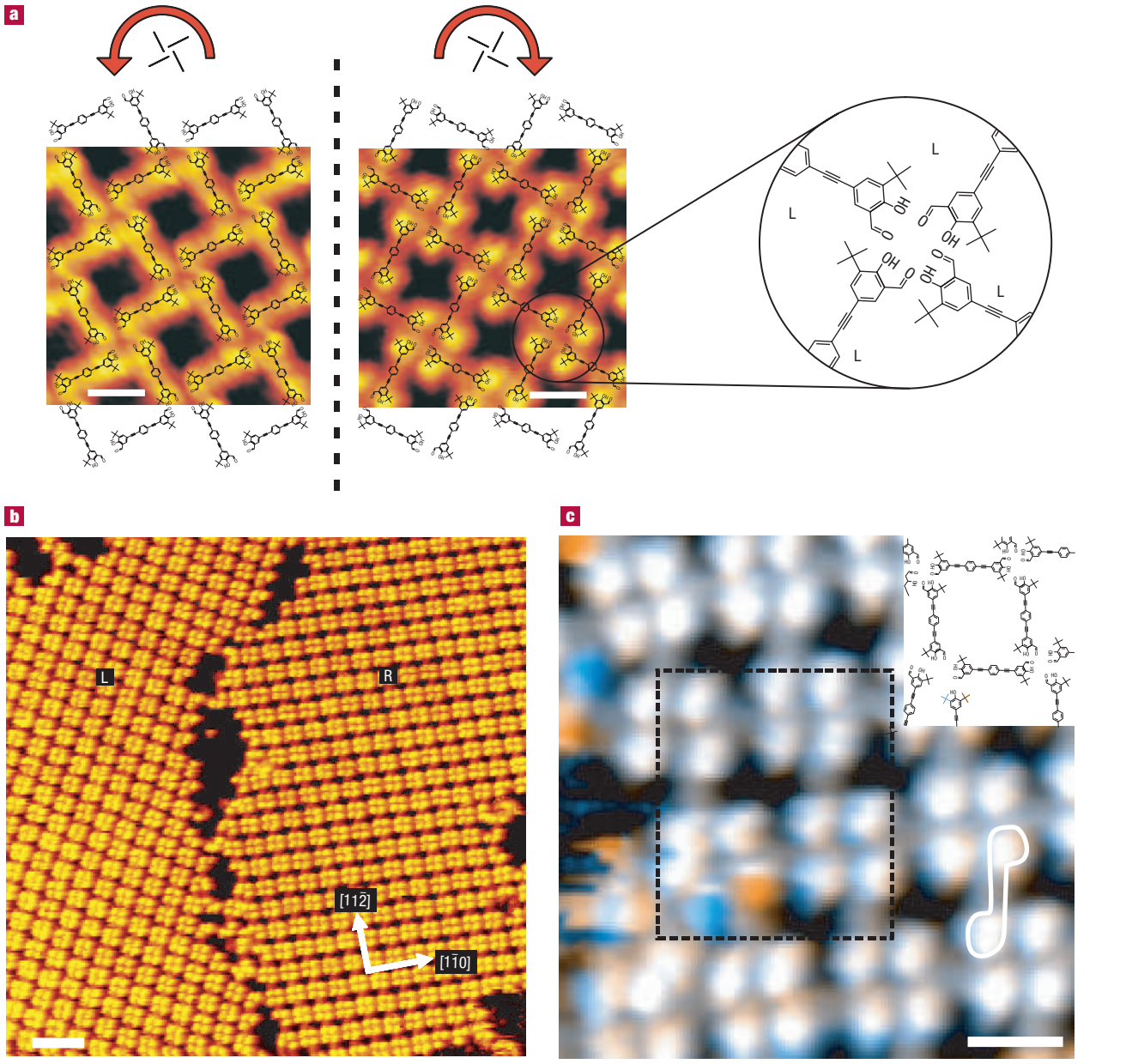

Figure 4 Network adsorption structure and chiral accommodation. a, STM images and schematic models of the network structure (scale bar 2 nm). The images show domains of opposite chirality, as seen from the sense of rotation for the chiral windmill motif, and have been obtained in imaging modes revealing the molecular π-systems and *t*-butyl groups, respectively. The zoom-in on a structural node illustrates the correlation between the tiling pattern and the molecular chirality, leading to homochiral domains consisting exclusively of RR or LL- conformers. **b**, Large-scale STM image (tunnel current 0.55 nA, sample voltage 1.25 V, scale bar 5 nm) showing two homochiral domains of opposite chirality. **c**, Overlay of two STM images visualizing the accommodation of an RL conformer at the boundary of an RR domain by a molecular conformational change (tunnel current 0.66 nA, sample voltage 1.25 V, time separation 19 s, scale bar 2 nm). Inset: the molecular structure in the area marked by a dashed square, including initial (blue) and final (orange) positions of the *t*-butyl group that moves.

argon-ion sputtering at 1.5 kV followed by annealing to 850 K, resulting in a well-ordered herringbone ($22 \times \sqrt{3}$) reconstruction. The molecules were synthesized as described in ref. 22 and were evaporated onto a substrate held at room temperature by vapour deposition from a heated quartz crucible. The STM was cooled with liquid nitrogen, and the STM images and videos were acquired during a gradual reheating of the sample to temperatures in the range 150–220 K. A typical STM video contains 100–300 images of a 15 nm × 15 nm area taken with an image-acquisition time in the range 6–20 s. All videos were acquired with a tunnelling resistance in the GΩ-range to make possible influences from the STM tip negligible. The STM videos were analysed by noting the number of *cis–trans* and *trans–cis* transitions, respectively, occurring between consecutive images. The transition rates $\Gamma_{trans–cis}$ and $\Gamma_{cis–trans}$ were subsequently determined from expressions derived from rate equations describing the two-level problem illustrated in Fig. 2b. This approach fully takes into account the possible occurrence of several flips between the moments in time when the tip visits the same position in consecutive images.

Theoretical modelling of molecule surface interactions was performed using the plane-wave-based DACAPO code[24,25] with the PW91 exchange correlation potential, an energy cutoff of 25 Ryd and periodic boundary conditions. The structures were modelled in a three-layer slab of the unreconstructed Au(111) surface using a 3 × 3 unit cell. Test calculations with a 3 × 4 unit cell, that is, increased intermolecular distance between the periodic

images, resulted in 0.003 eV higher binding energies, showing that the smaller unit cell already yields converged values. Long-range dispersive forces are only partly described in the current density functional theory setup. As the effect of such forces is presumably larger for the flat-lying molecule ends than for the molecule ends in the upright transition-state configuration, the calculated energy barrier is expected to increase slightly on improvement of the description of these forces. However, other effects not included in the calculations such as molecule–surface vibrations might counteract this by a comparable amount. Calculations for the entire free molecule were performed within the self-consistent charge density-functional-based tight-binding (SCC-DFTB) method[26].

Received 5 September 2005; accepted 21 November 2005; published 15 January 2006.

References

1. Yokoyama, T., Yokoyama, S., Kamikado, T., Okuno, Y. & Mashiko, S. Selective assembly on a surface of supramolecular aggregates with controlled size and shape. *Nature* **413,** 619–621 (2001).
2. Theobald, J. A., Oxtoby, N. S., Phillips, M. A., Champness, N. R. & Beton, P. H. Controlling molecular deposition and layer structure with supramolecular surface assemblies. *Nature* **424,** 1029–1031 (2003).
3. Lin, N., Dmitriev, D., Weckesser, J., Barth, J. V. & Kern, K. Real-time single-molecule imaging of the formation and dynamics of coordination compounds. *Angew. Chem. Int. Edn* **41,** 4779–4783 (2002).
4. Yanagi, H. *et al.* Molecularly resolved dynamics for two-dimensional nucleation of supramolecular assembly. *Nano Lett.* **2,** 601–604 (2002).
5. Schunack, M. *et al.* Long jumps in the surface diffusion of large molecules. *Phys. Rev. Lett.* **88,** 156102 (2001).
6. Lauhon, L. J. & Ho, W. Single molecule thermal rotation and diffusion: Acetylene on Cu(001). *J. Chem. Phys.* **111,** 5633–5636 (1999).
7. Gimzewski, J. K. *et al.* Rotation of a single molecule within a supramolecular bearing. *Science* **281,** 531–533 (1998).
8. Jung, T. A., Schlittler, R. R. & Gimzewski, J. K. Conformational identification of individual adsorbed molecules with the STM. *Nature* **386,** 696–698 (1997).
9. Moresco, F. *et al.* Conformational changes in single molecules induced by scanning tunneling microscopy manipulation: A route to molecular switching. *Phys. Rev. Lett.* **86,** 672–675 (2001).
10. Loppacher, Ch. *et al.* Direct determination of energy required to operate a single molecule switch. *Phys. Rev. Lett.* **90,** 066107 (2003).
11. Qiu, X. H., Nazin, G. V. & Ho, W. Mechanisms of reversible conformational transitions in a single molecule. *Phys. Rev. Lett.* **93,** 196806 (2004).
12. Ortega Lorenzo, M., Baddeley, C. J., Muryn, C. & Raval, R. Extended surface chirality from supramolecular assemblies of adsorbed chiral molecules. *Nature* **404,** 376–378 (2000).
13. Kühnle, A., Linderoth, T. R., Hammer, B. & Besenbacher, F. Chiral recognition in dimerization of adsorbed cysteine observed by scanning tunnelling microscopy. *Nature* **415,** 891–893 (2002).
14. Lopinski, G. P., Moffatt, D. J., Wayner, D. D. M. & Wolkow, R. A. Determination of the absolute chirality of individual adsorbed molecules using the scanning tunnelling microscope. *Nature* **392,** 909–911 (1998).
15. Fang, H., Giancarlo, L. C. & Flynn, G. W. Direct determination of the chirality of organic molecules by scanning tunneling microscopy. *J. Phys. Chem. B* **102,** 7311–7315 (1998).
16. Weckesser, J., De Vita, A., Barth, J. V., Cai, C. & Kern, K. Mesoscopic correlation of supramolecular chirality in one-dimensional hydrogen-bonded assemblies. *Phys. Rev. Lett.* **87,** 096101 (2001).
17. Chen, Q. & Richardson, N. V. Enantiomeric interactions between nucleic acid bases and amino acids on solid surfaces. *Nature Mater.* **2,** 324–328 (2003).
18. Böhringer, M., Schneider, W.-D. & Berndt, R. Real space observation of a chiral phase transition in a two-dimensional organic layer. *Angew. Chem. Int. Edn* **39,** 792–795 (2000).
19. Brian France, C. & Parkinson, B. A. Naphto[2,3-a]pyrende forms chiral domains on Au(111). *J. Am. Chem. Soc.* **125,** 12712–12713 (2003).
20. Gothelf, K. V., Brown, R. S., Thomsen, A. & Nielsen, M. 1,4-Bis[(5-tert-butyl-3-formyl-4-hydroxyphenyl)ethynyl]benzene (synthesis). World patent 2004050231 (2004).
21. Parschau, M., Romer, S. & Ernst, K.-H. Induction of homochirality in achiral enatiomorphous monolayers. *J. Am. Chem. Soc.* **126,** 15398–15399 (2004).
22. McFadden, C. F., Cremer, P. S. & Gellman, A. J. Adsorption of chiral alcohols on "chiral" metal surfaces. *Langmuir* **12,** 2483–2487 (1996).
23. Lægsgaard, E., Besenbacher, F., Mortensen, K. & Stensgaard, I. A fully automated, timble-size scanning tunneling microscope. *J. Micros.* **152,** 663–669 (1988).
24. Hammer, B., Hansen, L. B. & Nørskov, J. K. Improved adsorption energetics within density-functional theory using revised Perdew-Burke-Ernzerhof functionals. *Phys. Rev. B* **59,** 7413–7421 (1999).
25. Bahn, S. R. & Jacobsen, K. W. An object-oriented scripting interface to a legacy electronic structure code. *Comp. Sci. Eng.* **4,** 56–66 (2002).
26. Frauenheim, Th. *et al.* A self consistent charge density functional based tight-binding method for predictive materials simulations in physics, chemistry and biology. *Phys. Status Solidi B* **217,** 41–62 (2000).

Acknowledgements

We acknowledge the financial support from the EU programs FUN-SMART and AMMIST, as well as from the Carlsberg Foundation, the Danish Technical Research Council and from the Danish Natural Science Research Council through funding for the iNANO centre. We thank A. H. Thomsen and M. Nielsen for synthesizing the molecules.
Correspondence and requests for materials should be addressed to T.R.L.
Supplementary Information accompanies this paper on www.nature.com/naturematerials.

Competing financial interests

The authors declare that they have no competing financial interests.